Physical Model Investigations of Pressure Distributions Next to Ships Passing Through a Lock

Nils B. Kerpen
Leibniz Universität Hannover
Franzius-Institute
for Hydraulic, Waterways and Coastal Engineering
kerpen@fi.uni-hannover.de

Daniel B. Bung
Leibniz Universität Hannover
Franzius-Institute
for Hydraulic, Waterways and Coastal Engineering
bung@fi.uni-hannover.de

Torsten Schlurmann
Leibniz Universität Hannover
Franzius-Institute
for Hydraulic, Waterways and Coastal Engineering
schlurmann@fi.uni-hannover.de

Abstract

Due to rising transport rates on a global scale, dimensions of ships and vessels keep constantly growing in order to enhance transport efficiency. Supporting infrastructure in harbors has to be adapted and optimized to new conditions. This paper considers and analyses the hydrodynamic processes of ship lock passage by means of large scale physical modeling. It focuses on the local, instantaneous pressure distributions in between the hull of the vessel and the adjacent lock walls and how pressure fluctuations affect the overall locking process since it is primarily influenced by the ship's navigational speed. The latter effect directly affects the duration of the locking process in total which is in the focus of economical interests of local harbor industry.

Keywords: Locking, Pressure distribution, Ship passage

1. Introduction

The river Weser connects the city of Bremen with the North Sea. It has been regularly dredged to enable navigation from the North Sea to inland harbors in Bremen for larger ships. Since the river Weser shows moderate tidal effects, inland harbors are connected by sea locks to assist navigational efforts and alleviate transshipments and logistics.

Pressure distributions next to ships generated by passage are determined and illustrated by means of a physical model of the harbor 'Industriehafen' in the city of Bremen. The prototype gate is about 33 m in width and the tide-influenced maximum water stage is approximately 13 m. The clearance around the ship is the predominant factor controlling the maximum ship velocity during the locking process.

2. Methodology

The physical model investigations are carried out in a 20 m long, 0.98 m wide and 1.0 m deep current flume in the hydraulic laboratory of Franzius-Institute in Hanover in a scale of 1:52 according to FROUDE's similitude (Figure 1).

Discharges are controlled by an IDM. An adjustable weir at the downstream end of the flume regulates the water depth in the outer harbor and mimics the water level variations in the lock chamber. The locking time is limited to the time frame resulting from sufficient tidal water stages due to decreasing under keel clearance. The objectives are to analyze the pressure distribution on the hull of the ships of varying idealized geometry while passing the lock and to investigate the ship's navigability in dependence of varying navigational speed (v = 0.1 m/s – 0.4 m/s) and load draft. Pressure distributions next to the vessel hull are measured by three pressure inducers. Water levels are measured by five water level follower (wafo). Vertical ship motions are measured by two distance lasers located bow and stern.

The concept of the experimental configuration is to install the ship at fixed locations in the current flume. The adjoining flow field is studied by means of steady-state physically simulated equivalent discharge rates in the model being generated by the ship's displacement and navigational speed under natural conditions. A specially designed mechanical mounting system enables six degrees of freedom (DOF) motions, i.e. three translations of surge, sway, heave, and the three rotations of roll, pitch, and yaw. However, only five motions, namely heave, pitch, surge, yaw and sway are measured and consequently analyzed in order to deduce critical conditions induced by the adjoining flow field.

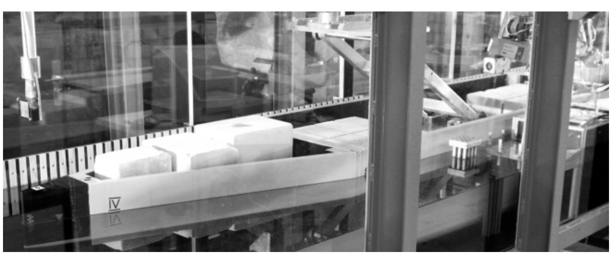

Figure 1. Physical model setup in scale of 1:52 at Franzius-Institute Hanover

3. Boundary Conditions

3.1. Tide influence

Due to the tide influence on the analyzed lock in Bremen a lock passage for ships according to Table 1 is only possible in a two-hour time frame during mean high water (MHW). In a save assumption the minimal water level during this two-hour time frame will be set constant in the physical model. Thus, the still water level (SWL) in the outer harbor (0.5 m deeper than the lock chamber) will be set to 11.8 m for ship 1 and 3; the SWL for ship 4 to 12.2 m.

3.2. Ship parameter

Dimensions of the analyzed ships are shown in Table 1. Ship 2 is not part of the investigations described in this paper.

Table 1. Ship parameters in prototype dimensions for physical model investigations (ship 2 is not part of the investigations described in this paper)

ship	dimension (*L* x *W* x *D*) [m]	UKC [m]
1	225.0 x 32.3 x 9.45	1.85
3	225.0 x 32.3 x 10.7	0.60
4	190.0 x 29.2 x 11.2	0.50

Ship 1 represents the present design ship. This ship is able to pass the outer lock gate with a mean velocity of 0.25 m/s. Ship 3 has the same geometry but will be analyzed with a larger draft. Ship 4 is not as long and wide as Ship 1 and 3 but has less under keel clearance (UKC).

To compare the results from the three different ship types shown in Table 1, a dimensionless parameter A_{block} is introduced representing the ratio of the ship's cross-sectional area A_S and the gate's cross-section area A_G:

$$A_{block} = A_S/A_G \ [-] \tag{1}$$

The parameter A_{block} (Table 2) arises out of a width of 35.1 m in the centerline of the outer lock gate and water levels according to Table 1 of 11.3 m for ship 1 and 3 and 11.6 m in the lock gate axis for ship 4.

Table 2. Dimensionless parameter A_{block} for ship's geometry in position 2 according to Table 1

	ship 1	ship 3	ship 4
A_{block}	0.77	0.87	0.79

4. Results

In order to appreciate the behavior of the pressure distribution next to the ship in the axis of the lock gate characteristics of water level variations between lock chamber and outer harbor have to be known as well as the ship's dynamics induced by this water level difference.

4.1. Water level variations

During ship's inbound process form the outer harbor into the lock chamber the water level in the lock chamber increases temporarily because of ship's displacement. The water level decreases in the lock chamber during the outbound analogous.

The cross section area in the lock gate axis, the back flow can pass through, is nearly completely blocked by the ship. The blocking factor A_{block} is listed in (Table 2). The water level increase during the inbound process is displayed in Figure 2 – Figure 4. Water level changes in the lock chamber are measured by wafo 1 and 2, changes in the outer harbor by wafo 4 and 5. Wafo 3 measures the water level in axis of the lock gate directly above the pressure inducers. Ship's position in the lock gate is displayed on the bottom of the figure, water level differences to the SWL in the lock chamber in an additional graph in the upper right corner of the figure.

The intensity of the water level increase in the lock chamber depends on the inbound velocity and ships position. The most dominant increase can be documented for position 2 because in this position the cross section area in the lock gate axis is blocked most intensive. On this account A_{block} (Table 2) is defined in this position.

To compare the results from all three analyzed ships, water levels from ship 1 and 3 in position 2 are displayed in Figure 5 and Figure 6. It can be seen that ship 3 (with greatest factor A_{block}) reveals the most intensive water surface elevation in the lock chamber.

Figure 7 presents the outbound of ship 1 in position 2. The water level decrease in the lock chamber (in this figure wafo 4 and 5) is more dominant than the increase during the inbound (Figure 3) because this effect reveals in a fall of ship's stern and reduces the cross section area for the back flow.

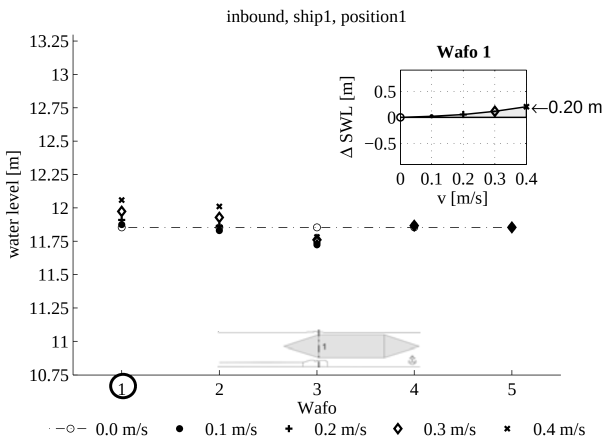

Figure 2. Water levels in outer harbor and lock chamber for different ship velocities (ship 1, position 1, inbound)

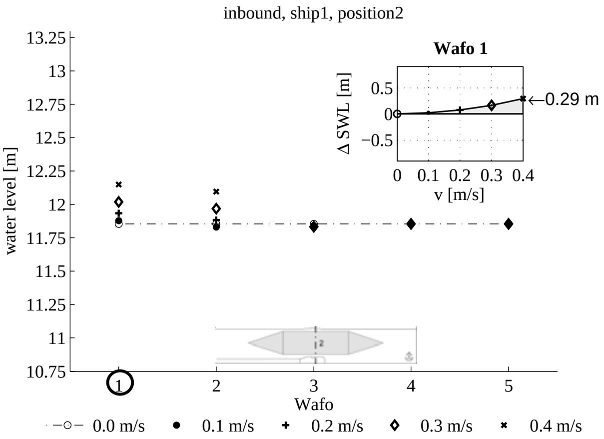

Figure 3. Water levels in outer harbor and lock chamber for different ship velocities (ship 1, position 2, inbound)

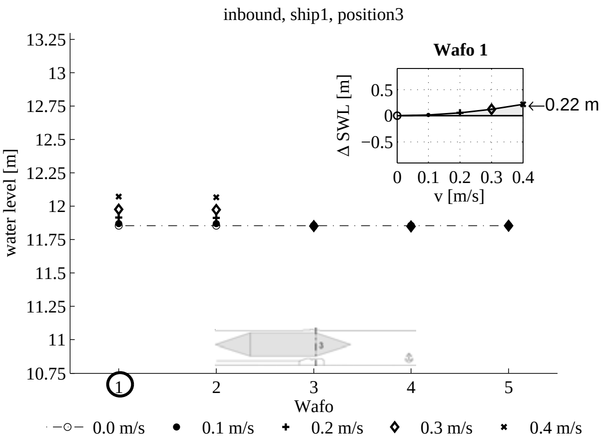

Figure 4. Water levels in outer harbor and lock chamber for different ship velocities (ship 1, position 3, inbound)

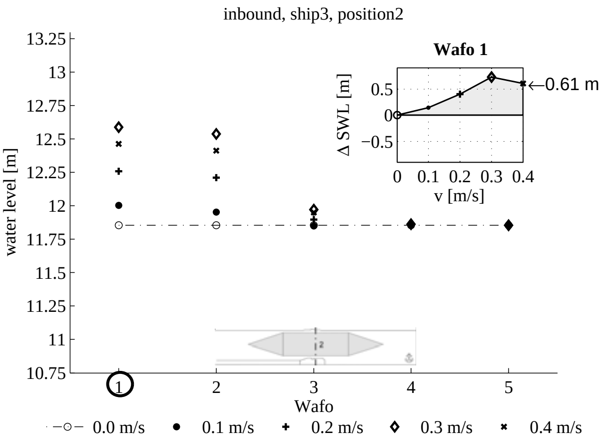

Figure 5. Water levels in outer harbor and lock chamber for different ship velocities (ship 3, position 2, inbound)

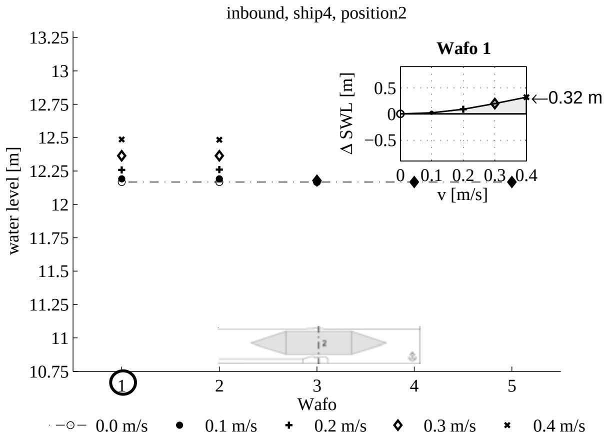

Figure 6. Water levels in outer harbor and lock chamber for different ship velocities (ship 4, position 2, inbound)

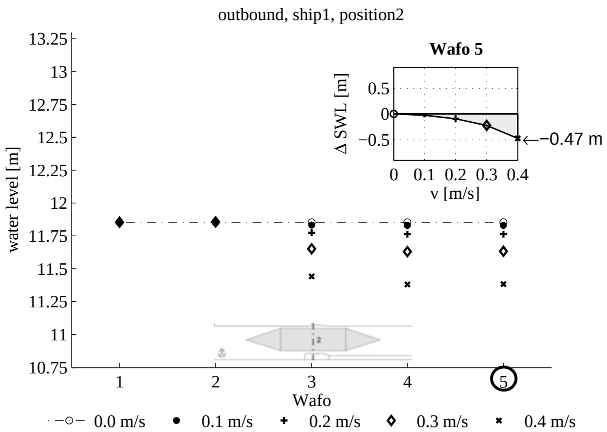

Figure 7. Water levels in outer harbor and lock chamber for different ship velocities (ship 1, position 2, outbound)

4.2. Ship’s motion

Figure 8 and Figure 9 show exemplarily the keel position of ship 4 in position 2 during in- and outbound. Two additional graphs on the top of the figure show the remaining UKC bow and stern for all analyzed passing velocities. In both figures passing direction is from right to left.

During inbound process (Figure 8) the water volume in the lock chamber is replaced by the ship. This reveals in a rising water level in the lock chamber (Figure 6) and thereby in a bow elevation and an increasing UKC. The intensity depends on the inbound velocity.

During the outbound process (Figure 9) the water volume in the lock chamber is ‘decompressed’ by the ship. The water level in the lock chamber is falling, stern is declining and the UKC is decreasing. With an outbound velocity of 0.3 m/s and 0.4 m/s the stern hits the ground.

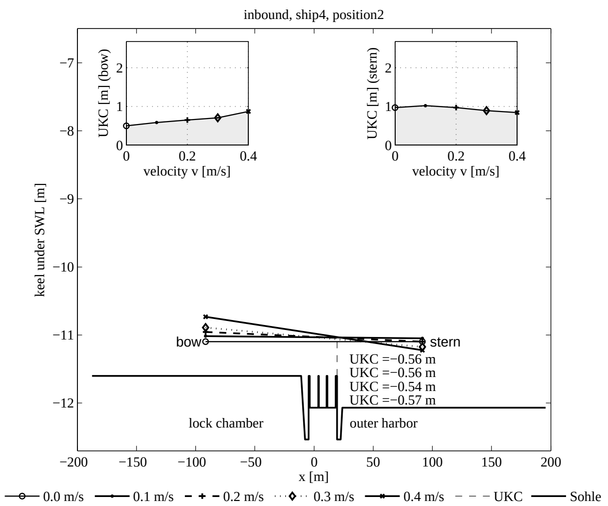

Figure 8. Keel position during inbound process of ship 4, position 2 with remaining UKC for different ship velocities

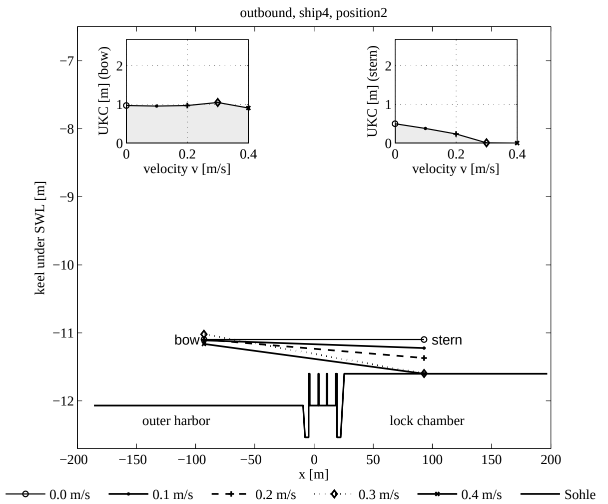

Figure 9. Keel position during outbound process of ship 4, position 2 with remaining UKC for different ship velocities

4.3. Pressure distributions

Bed related hydraulic energy head can be described as the sum of potential energy head and velocity head. BERNOULLI equation describes this energy head h_E of a frictionless fluid in a steady state flow without energy losses on one horizontal level for idealized 1D flow by

$$h_E = p/(\rho \cdot g) + v^2/(2 \cdot g)\,. \tag{2}$$

The vertical pressure distributions [m H_2O] between ship hull and lock gate at wafo 3 according to the four measured ship velocities are shown in Figure 10 – Figure 12. Pressures are plotted on the x-axis and the dedicated water depth on the y-axis. The hydrostatic pressure distribution under SWL is represented by the dash-dot line. Two detailed graphs enable a closer look to the pressure distributions under the water surface (detail A) and near the floor (detail B).

Detail A indicates a pressure rise with an increasing inbound velocity. The water depth is increasing, because of an increasing water level in the lock chamber (Figure 4). All detected pressures are higher than the hydrostatic pressure under SWL. The pressure increase in point A is caused in the narrow cross section geometry, the water can pass through. The water flows from the lock chamber into the outer harbor because of an increased water level in the lock chamber. Flow velocity in this point is slow (observation), thus the pressure increases.

Near the ground geometry (detail B) pressures increase not as intensive as at point A. Pressures are lower than the hydrostatic pressure under SWL even though the water level increases. This observation can be explained by the cross section area available to the water flow as well. In the cross section area located in the lock gate axis most space is given to the return current by the UKC. Hence, the velocities increase in this area and the pressures decrease according to equation (2).

Pressure distributions for ship 1 indicate the same system performance (Figure 11). The intensity is not as high as for ship 3 because the UKC is more than three times higher (Table 1). Hence, the water level in the lock chamber is not increasing as intensive as for the inbound of ship 3 (Figure 4, Figure 5).

Pressure distributions for ship 4 indicate smaller pressures near the water surface (Point A) because of a smaller ship width (Table 1) and hence, due to an increased cross section area in point A.

Concluding, the measured pressures in Figure 10 and observed velocity distributions reflect the interrelationship of potential end kinetic energy described by equation (2). The pressure distributions deviate from the hydrostatic pressure in dependence of the available cross section area. Deviations can although be observed for a single velocity in different water depth.

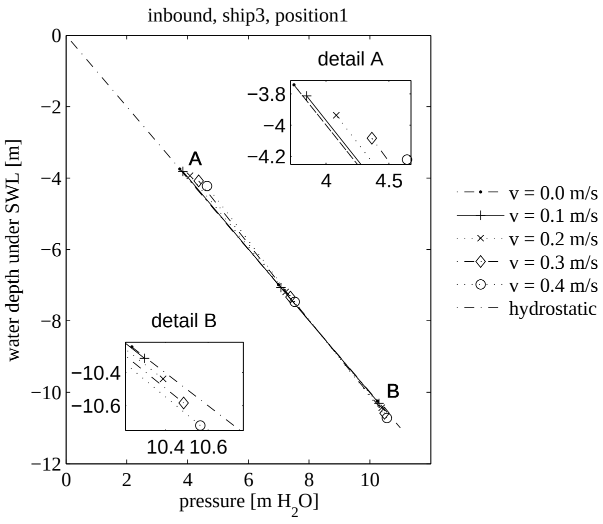

Figure 10. Vertical pressure distributions between ship hull and lock gate (inbound, ship 3, position 1)

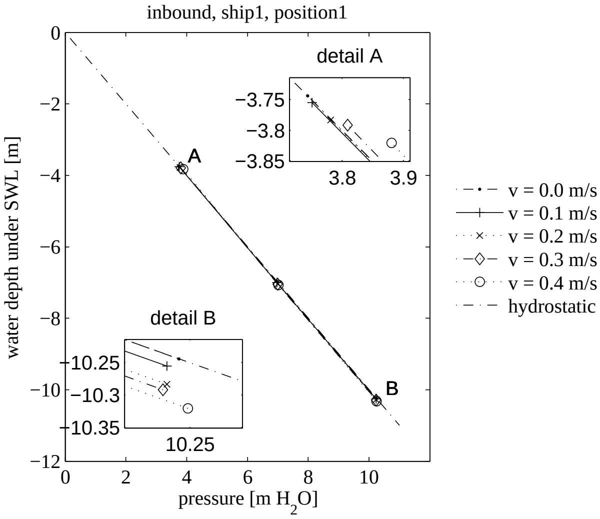

Figure 11. Vertical pressure distributions between ship hull and lock gate (inbound, ship 1, position 1)

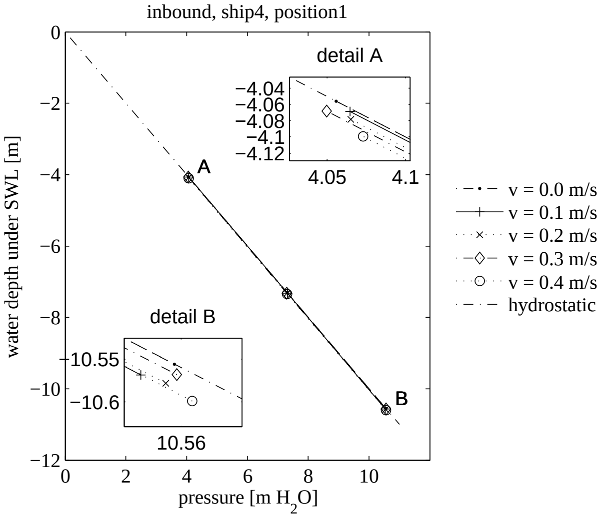

Figure 12. Vertical pressure distributions between ship hull and lock gate (inbound, ship 4, position 1)

5. Conclusion

Critical structural configurations and combinations for the design ship passage in the sea lock are analyzed and pointed out. It has been proved that the design case for the actual passing design ship (Table 1, ship 1) is reproducible and hence, the results can be transferred to prototype scale.

The intensity between water level difference in the lock chamber and the outer harbor depends on ship's velocity and position during in- and outbound process on the one hand and on the factor A_{block} on the other hand. If the dimensionless parameter A_{block} becomes too large (ship 3), a passage of the lock gate is not possible.

Primarily, these water level differences which are affected by the ship's in- and outbound velocity lead to ship's vertical bow and stern motion.

A deviation from hydrostatic pressure distribution along the water column could be detected for ships in narrow spaced channels like lock gates physically based in the BERNOULLI equation. This deviation finally depends on the spacing around the ship hull and thereby again on the factor A_{block}.

6. References

[1] M. J. Briggs, "Ship Squat Predictions for Ship/Tow Simulator" *US Army Corps of Engineers, Engineering,* Research and Development Center 3909 Halls Ferry road Vicksburg, MS 39180-6199, 2006, pp. 2-13

[2] G. Bollrich, *Technische Hydromechanik 1*, Verlag Bauwesen, Vol. 5, 2000, pp. 111-124

[3] Bremenorts, *Industriehafen Bremen*, bremenports Gmbh & Co.KG, 2nd edition, 2006